GABA-mediated giant depolarizing potentials as coincidence detectors for enhancing synaptic efficacy in the developing hippocampus

Alexander M. Kasyanov*, Victoria F. Safiulina*†, Leon L. Voronin†, and Enrico Cherubini*‡

*Neuroscience Programme, International School for Advanced Studies, 34014 Trieste, Italy; and †Institute of Higher Nervous Activity and Neurophysiology, Russian Academy of Sciences, Butlerova 5a, 117485 Moscow, Russia

Edited by Per O. Andersen, University of Oslo, Oslo, Norway, and approved January 14, 2004 (received for review September 16, 2003)

Spontaneously occurring neuronal oscillations constitute a hallmark of developmental networks. They have been observed in the retina, neocortex, hippocampus, thalamus, and spinal cord. In the immature hippocampus, the so-called ''giant depolarizing potentials'' (GDPs) are network-driven synaptic events generated by γ-aminobutyric acid (GABA), which at this stage is depolarizing and excitatory. We have tested the hypothesis that during the first postnatal week, GDP-associated calcium signals may alter the properties of synaptic transmission at poorly developed mossy fiber (MF)–CA3 connections. We found that ''pairing'' GDPs with MF stimulation induced a persistent increase in synaptic efficacy at MF–CA3 synapses. When the interval between GDPs and MF stimulation was increased, the potentiating effect progressively declined and disappeared. The potentiation depended on activation of voltage-dependent calcium channels and calcium flux. This activity may contribute to the refinement of neuronal connectivity before the establishment of the adult neuronal circuit.

mossy fibers | synaptic plasticity | GABA-mediated oscillatory events | development | synaptic pairing

Giant depolarizing potentials (GDPs) are network-driven membrane oscillations characterized by recurrent membrane depolarization with superimposed fast action potentials. Usually, they last hundreds of milliseconds and are separated by intervals of several seconds (1). They have been recorded also in the intact brain of rat pups, where they occur at the same frequency as in acute slices (0.3–0.1 Hz) during immobility periods, sleep, and feeding (2). GDPs depend on the synergistic action of γ-aminobutyric acid (GABA) and glutamate acting on $GABA_A$ and (RS)-α-amino-3-hydroxy-5-methyl-4-isoxadepropionate (AMPA) receptors, respectively (1, 3). Early in postnatal life, GABA depolarizes and excites the postsynaptic cells (4–6) because of high intracellular $[Cl^-]$, which results mainly from the unbalance of two Cl^- cotransporter systems, the NKCCl and KCC2 that enhance and lower intracellular $[Cl^-]$, respectively (7). Unlike adult neurons in immature cells, the reversal potential for GABA (E_{GABA}), which is set by the electrochemical gradient for Cl^-, the main anion permeating GABA receptor channels, is more positive than the resting membrane potential. GDPs disappear toward the end of the first postnatal week, when GABA becomes inhibitory (1) because of a developmental shift of E_{GABA} toward more hyperpolarized potentials. This results from changes in the expression of the K^+/Cl^- cotransporter KCC2 (8). This switch appears to be regulated by GABA because it can be prevented by blocking $GABA_A$ receptors and accelerated by increasing $GABA_A$ receptor activation (9), thus suggesting a prominent role of GABA signaling during postnatal development (10). The depolarizing action of GABA during GDPs results in calcium influx through the activation of *N*-methyl-D-aspartate (NMDA) receptors and voltage-dependent calcium channels (11–13). Thus, as in many others developing systems (14–17), GDPs ensure large calcium oscillations even in neurons with few synapses (6, 13).

Calcium signaling may alter the properties of synaptic transmission, contributing to the structural refinement of neuronal connectivity and to the establishment of the adult neuronal circuit (18). Hence, after their initial formation, synaptic connections undergo profound remodeling with elimination of some and strengthening of others (18). The rewiring would depend on electrical activity involving cooperative and competitive interaction between converging inputs (18, 19). In accord with the Hebb postulate on activity-dependent synaptic strengthening, here the hypothesis has been tested that GDPs may act as coincident detector signals between pre- and postsynaptic activity. This assumption has been verified on mossy fiber (MF)–CA3 connections that, during the first postnatal week, are still poorly developed, reaching a full maturation only toward the end of the second postnatal week (20). This pathway is of particular interest because it can release GABA in addition to glutamate (21). Moreover, it has been shown that, during postnatal development, granule cells of the dentate gyrus (DG), from which MF originate, transiently express a functional GABAergic phenotype (22).

Methods

Slice Preparation. Experiments were performed on hippocampal slices obtained from postnatal day 1 (P1)–P6 Wistar rats as described (23). Briefly, animals were decapitated after being anaesthetized with an i.p. injection of urethane (2 g/kg). All experiments were carried out in accordance with the European Community Council Directive of 24 November 1986 (86/609EEC) and were approved by local authority veterinary service. The brain was quickly removed from the skull and placed in ice–cold artificial cerebrospinal fluid (ACSF) containing 130 mM NaCl, 3.5 mM KCl, 1.2 mM NaH_2PO_4, 25 mM $NaHCO_3$, 1.3 mM $MgCl_2$, 2 mM $CaCl_2$, and 25 mM glucose, and saturated with 95% O_2 and 5% CO_2 (pH 7.3–7.4). Transverse hippocampal slices (500 μm thick) were cut with a vibratome and stored at room temperature in a holding bath containing the same solution as above. After a recovery period of at least 1 h, an individual slice was transferred to the recording chamber, where it was continuously superfused with oxygenated ACSF at a rate of 2–3 ml/min at 33–34°C.

Electrophysiological Recordings. Electrophysiological experiments were performed from CA3 pyramidal cells by using the whole-

This paper was submitted directly (Track II) to the PNAS office.

Abbreviations: GABA, γ-aminobutyric acid; CPP, α-3-(2-carboxy-piperazin-4-yl)-propyl-1-phosphonic acid; CV, coefficient of variation; D-AP5, D-(−)-2-amino-5-phosphonopentanoic acid; DCG-IV, (2S,2′R,3′R)-2–2(2′,3′-dicarboxycyclopropyl) glycine; EPSC, excitatory postsynaptic current; GDPs, giant depolarizing potentials; LAP-4, 2-amino-4-phosphonobutyric acid; LTP, long-term potentiation; MF, mossy fibers; NMDA, *N*-methyl-D-aspartate; VDCC, voltage-dependent calcium channels; DG, dentate gyrus; BAPTA, 1,2-bis(2-aminophenoxy)ethane-*N*,*N*,*N*′,*N*′-tetraacetic acid; P*n*, postnatal day *n*.

‡To whom correspondence should be addressed. E-mail: cher@sissa.it.

cell configuration of the patch-clamp technique in current or voltage-clamp mode. Synaptic currents were evoked (from a holding potential of −70 mV) at 0.1 Hz by minimal stimulation of MF in stratum lucidum using bipolar twisted NiCr-insulated electrodes. The stimulus strength was adjusted to reliably activate only one or few presynaptic fibers with a constant latency within <1 ms. Responses were associated with transmitter failures. These were considered true transmitter failures and not failures in activating presynaptic fibers because, on average, the amplitude of a second response, following the first with 50-ms delay, was similar whether or not this was preceded by a failure or a success (in 10 neurons the mean amplitude of the second response occurring after failures or successes was 9.3 ± 4.5 pA and 8.9 ± 4.8 pA, respectively). This indicates that, in the majority of the cases, the action potential did not fail to invade the axon terminal. In most cases, paired stimuli were applied at 50-ms interval. Latency did not change when two pulses in the paired-pulse paradigm were applied, and therefore synaptic responses were supposed to be monosynaptic. In three experiments, multifiber responses were evoked at 0.1 Hz in CA3 pyramidal cells (using higher stimulus strength) by stimulating electrodes placed in the DG. We did not routinely use this protocol because, usually in neonatal rat, this induces the activation of GDPs. Responses were considered as generated by MF on the basis of their sensitivity to group II and III metabotropic glutamate receptor agonists (2S,2′R,3′R)-2–2(2′,3′-dicarboxycyclopropyl) glycine (DCG-IV, 1 μM) and 2-amino-4-phosphonobutyric acid (LAP-4, 10 μM), respectively (24, 25). They were also considered as generated by MF on the basis of their strong paired-pulse facilitation and frequency facilitation (see ref. 26). In some experiments, two different inputs converging on the same neuron were alternatively activated at 0.2 Hz by placing the stimulating electrodes in stratum lucidum and stratum radiatum, to activate MF or GABAergic terminals, respectively (Fig. 1*A*). It should be stressed that, in the immediate postnatal period, GABAergic interneurons innervating mainly the apical dendrites of pyramidal neurons are located in stratum radiatum, whereas collateral from other CA3 pyramidal neurons are still poorly developed (27). GABAergic inputs (from interneurons) were identified on the basis of their insensitivity to LAP-4 and their ability to be blocked by picrotoxin.

Patch electrodes were pulled from borosilicate glass capillaries (Hingelberg, Malsfeld, Germany). They had a resistance of 5–7 MΩ when filled with an intracellular solution containing 115 mM K-gluconate, 20 mM KCl, 10 mM disodium phosphocreatine, 10 mM Hepes, 4 mM MgATP, and 0.3 mM GTP. In some ($n = 9$) experiments, recordings were performed with patch pipettes containing the calcium chelator 1,2-bis(2-aminophenoxy)ethane-*N*,*N*,*N*′,*N*′-tetraacetic acid (BAPTA, 20 mM, purchased from Sigma).

Recordings were made with a patch clamp amplifier (Axopatch 1D; Axon Instruments). The whole cell capacitance was fully compensated and the series resistance (10–20 MΩ) was compensated at 75–80%. The stability of the patch was checked by repetitively monitoring the input and series resistance during the experiment. Cells exhibiting 15–20% changes were excluded from the analysis. After a control period of 5–10 min, the patch was switched from voltage-clamp to current-clamp mode and MF responses were paired for 5 min with GDPs. "Pairing" consisted in triggering MF stimulation with the rising phases of GDPs (Fig. 1*B*). After this period the patch was switched back to voltage clamp mode and synaptic currents were recorded as in control. When two stimuli were alternatively applied to two different inputs, only one was paired whereas the other input was not stimulated during this period.

Drugs used were α-3-(2-carboxy-piperazin-4-yl)-propyl-1-phosphonic acid (CPP), D-(−)-2-amino-5-phosphonopentaoic acid (D-AP5), DCG-IV, LAP-4, picrotoxin, all purchased from Tocris Cookson (Bristol, U.K.); and nifedipine, purchased from Sigma. All drugs were dissolved in artificial cerebrospinal fluid, except picrotoxin, which was dissolved in DMSO. The final concentration of DMSO in the bathing solution was 0.1%. At this concentration, DMSO alone did not modify the shape or the kinetics of synaptic currents. Drugs were applied in the bath via a three-way tap system, by changing the superfusion solution to one differing only in its content of drug(s). The ratio of flow rate to bath volume ensured complete exchange within 2 min.

Data Acquisition and Analysis. Data were stored on a magnetic tape and transferred to a computer after digitization with an A/D converter (Digidata 1200, Axon Instruments, Foster City, CA). Data acquisition was done by using PCLAMP (Axon Instruments) and LTP114 software package (courtesy of W. W. Anderson, Bristol University, Bristol, U.K.). Data were sampled at 10 kHz and filtered with a cutoff frequency of 1 kHz.

Mean excitatory postsynaptic current (EPSC) amplitude was obtained by averaging successes and failures. Paired-pulse ratio was calculated as the ratio between the mean amplitude of EPSC2 over EPSC1. The coefficient of variation (CV) of response amplitude was determined as the ratio between standard deviation and mean and its inverse squared value (CV^{-2}) was calculated.

Values are given as mean ± SEM. Significance of differences was assessed by Student's *t* test or Wilcoxon signed rank test. Significance level, $P < 0.05$.

Results

Identification of MF Responses. In accord with previous work (1), whole cell recordings in current clamp mode from 65 CA3 pyramidal neurons at P1–P6 revealed the presence of GDPs (Fig. 1*B*) whose frequency varied from 0.06 to 0.47 Hz (0.092 ± 0.009 Hz; mean ± SEM here and below). We used a "pairing" procedure to correlate GDPs with MF activation. For this purpose, the rising phase of a GDPs was used to trigger MF stimulation in stratum lucidum in such a way that spontaneous GDP activity was coincident with presynaptic activation of MF (see enlargement of Fig. 1*B*). Before pairing, synaptic currents were evoked in voltage clamp conditions by minimal stimulation of MF in stratum lucidum at 0.1 Hz from a holding potential of −70 mV. Synaptic currents were associated with response failures. Synaptic responses were generated by MF as indicated by their sensitivity to group II and III metabotropic glutamate receptors (mGluR) agonists DCG-IV (1 μM) and LAP-4 (10 μM, Fig. 1*C*) (24, 25). On average, DCG-IV induced a reduction in EPSC amplitude of 40 ± 17% ($n = 5$), whereas LAP-4 induced a reduction of 70 ± 13%, ($n = 17$). The weaker effect of DCG-IV in comparison to LAP-4 may be due to developmental differences between group II and III mGluRs expression. MF-induced synaptic currents were also characterized by their strong paired-pulse facilitation, when two closely spaced stimuli (with 50-ms interval) were delivered to stratum lucidum (26). LAP-4-sensitive synaptic currents were also completely abolished by picrotoxin (100 μM, Fig. 1*C*), suggesting that, early in development, the vast majority of mossy fibers release GABA (see also ref. 22). DNQX (6,7-dinitroquinoxaline-2,3-dione)-sensitive synaptic responses could appear in the presence of picrotoxin by increasing stimulation intensity (two times or more). It is likely that the increased stimulus strength recruited additional fibers (belonging to MF or to associative-commissural fibers) that produced synaptic responses mediated by glutamate acting on (RS)-α-amino-3-hydroxy-5-methyl-4-isoxadepropionate (AMPA) type of receptors. Multifiber responses elicited by stimulation of the DG exhibited strong paired-pulse facilitation and frequency facilitation ($n = 3$). The paired pulse ratio was 2.7 ± 0.6. Changing the frequency of stimulation from 0.05 Hz to 0.3 Hz, resulted in a reversible increase in amplitude of the

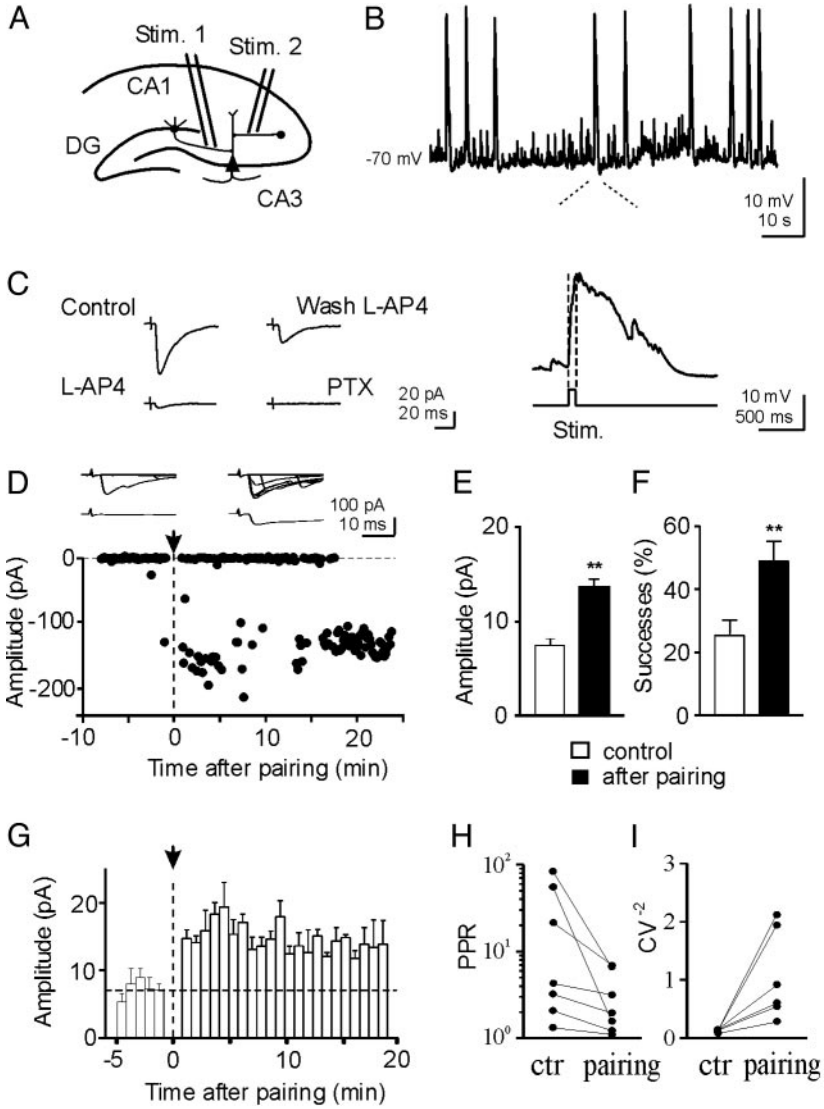

Fig. 1. Pairing GDPs with MF stimulation persistently enhances synaptic efficacy at MF-CA3 synapses. (*A*) Diagram of the hippocampus showing a CA3 pyramidal cell with two converging inputs: one from MF (Stim. 1), the other from GABAergic interneurons (Stim. 2). (*B*) GDPs recorded from a CA3 cell in current clamp mode from the hippocampus of a P3 old rat. Below the trace, a single GDP is shown on an expanded time scale. Note the absence of spikes riding on the top of GDP due to block of the sodium channel with QX 314. The rising phase of GDPs (between the dotted lines) was used to trigger synaptic stimulation (Stim). (*C*) Typical MF response recorded in control conditions (Control), after adding 10 μM of LAP-4 to the bathing solution (LAP-4), after washing out LAP-4 (Wash LAP-4), and after adding 100 μM picrotoxin (PTX). Each response is the average of 30 trials (including failures). (*D*) Amplitudes of synaptic responses (dots) evoked by stimulation of MF before and after pairing (arrow at time 0) are plotted against time. The traces above the graph represent 7 individual responses evoked before (*Left*) and 15 min after pairing (*Right*); lower traces represent the average of 48 individual responses (successes and failures) obtained before (*Left*) and 15 min after pairing (*Right*). (*E* and *F*) Mean EPSC amplitude (*E*) and mean percentage of successes (*F*) for 20 P1–P6 CA3 pyramidal neurons examined before (white column) and 15 min after pairing (black column). (*G*) Summary plot of mean EPSC amplitude versus time for 20 cells. Each column represents the mean response amplitude from five trials (50 s). Bars represent the SEM. (*H* and *I*) Paired-pulse ratio and CV^{-2} calculated before (ctr) and 15 min after pairing. After pairing, the mean paired-pulse ratio and CV^{-2} were significantly different from control ($P < 0.05$).

synaptic responses up to 329 ± 8%, suggesting that they were mediated by MF inputs (Fig. 5, which is published as supporting information on the PNAS web site; see also ref. 26).

Pairing GDPs with MF Activation Enhances Synaptic Efficacy. After response stabilization (5–10 min of control), the patch was switched from voltage-clamp to current-clamp mode and MF responses were paired for 5 min with GDPs. The mean number of GDPs occurring in 59 cells during this period was 27.6 ± 2.7. As shown in Fig. 1*D*, this procedure produced a strong and persistent potentiation of MF-mediated synaptic currents (from 0.4 ± 1.8 pA to 104.8 ± 6.9 pA in 48 trials before and 15 min after pairing, respectively). Average data are illustrated in Fig. 1*E*. The amplitude enhancement was associated with a significant increase in the number of successes (from 25 ± 5% to 49 ± 6%, Fig. 1*F*). The effects of pairing were long lasting (up to 30 min; Fig. 1 *D* and *G*). In double pulse experiments ($n = 7$), long-term potentiation (LTP) was associated with a significant reduction in the paired-pulse ratio (from 24.4 ± 12.3 to 3.2 ± 0.9; $P < 0.05$) and a significant increase in the inverse squared value of the coefficient of variation (CV^{-2}) of response amplitude (from 0.09 ± 0.03 to 1.1 ± 0.3; $P < 0.05$; $n = 6$; Fig. 1 *H* and *I*). This suggests that an increased probability of transmitter release accounts for LTP expression. In 20 cells, 15 min after pairing the mean amplitude increase in synaptic currents was 185 ± 13%; $P < 0.001$ (Fig. 1*G*). Three neurons could be considered

"presynaptically silent" because they exhibited no responses to the first pulse but occasional responses to the second pulse occurring with 50-ms delay after the first (Control in Fig. 6, which is published as supporting information on the PNAS web site; see refs. 23, 28, and 29). The pairing protocol caused the appearance of responses to the first stimulus (Fig. 6) and increased the number of successes to the second one. Pairing-induced potentiation of MF responses was not related to the spikes riding on the top of GDPs because all experiments were performed with an intrapipette solution containing QX 314, which is known to block sodium channels.

Pairing multifiber responses with GDPs induced a strong and persistent potentiation of synaptic currents (from 19. 5 ± 4.6 pA to 51.7 ± 8.8 pA before and 15 min after pairing, respectively; Fig. 7, which is published as supporting information on the PNAS web site). As for single-fiber responses, this effect was associated with a reduction in paired-pulse ratio (from 2.7 ± 0.6 to 0.6 ± 0.2 before and after pairing, respectively). Differences in the paired pulse ratio between composite and single fiber responses can be attributed to the fact that the latter include cases with very low probability of successes to the first pulse in the paired pulse paradigm and therefore with very high paired-pulse facilitation ratio.

In one neuron synaptic currents probably originating from a GABAergic interneuron (they were insensitive to LAP-4 but were abolished by picrotoxin) were potentiated by GDPs (the mean amplitude of the synaptic response was 4.5 ± 1.3 pA and 10.7 ± 2.5 pA, before and 10 min after pairing, respectively). This suggests that pairing-induced potentiation is a more general phenomenon nonrestricted exclusively to MF inputs (Fig. 8, which is published as supporting information on the PNAS web site).

In the absence of pairing, no significant changes in synaptic efficacy could be detected ($n = 5$; Fig. 2 *A* and *B*; $P > 0.5$). "No pairing" consisted in switching the patch for 5 min from voltage clamp to current clamp mode. In this period, GDPs occurred randomly in the absence of afferent stimulation. In these cells, the mean peak amplitude current was 7.0 ± 2.5 pA and 8.2 ± 2.7 pA in control and 20 min after switching from current-clamp to voltage-clamp conditions, respectively. Similarly, success rate varied from 57 ± 8% to 56 ± 13%.

The temporal specificity of pairing required for LTP induction was tested in 38 cells by introducing a delay between GDPs and synaptic stimulation. The delay was varied between 0 and 5 s. As shown in Fig. 2*C*, a maximum effect was achieved when pre- and postsynaptic signals were coincident. Synaptic potentiation declined to reach the control level (100%) when presynaptic signals were activated 2–3 s after GDPs. The amplitude of synaptic responses obtained with a delay >3.5 s was significantly ($P < 0.05$) different from that obtained with coincident stimulation.

GDP-Induced Potentiation Is Restricted to the Paired Input. One interesting question is whether GDP-induced increase in synaptic strength is restricted to the activated synapse or whether it spreads to other adjacent nonactivated (unpaired non-MF) inputs converging on the same CA3 pyramidal cell. In another set of experiments ($n = 8$), two different inputs converging onto the same postsynaptic cell were alternately activated (see diagram of Fig. 1*A*). After a control period of 5–10 min, the pairing procedure was applied to only one input. At the end of the experiments, the origin of presynaptic fibers was pharmacologically identified with LAP-4 and picrotoxin. In the example of Fig. 3, synaptic responses induced by stimulation of one electrode (Stim. 1) exhibited paired-pulse facilitation, whereas the other (Stim. 2) exhibited paired-pulse depression (Fig. 3 *A* and *B*). Pairing input 1 with GDPs led to a persistent enhancement of synaptic efficacy of this input (Fig. *3*A), but not input 2, which remained unchanged (Fig. 3*B*). Pharmacological identification

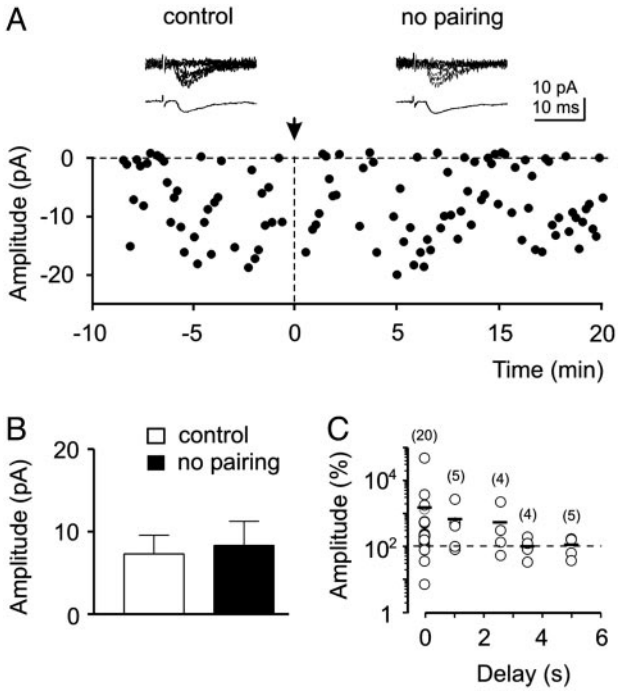

Fig. 2. Lack of potentiation in unpaired neurons. (*A*) The amplitude of synaptic currents (filled circles) evoked by MF stimulation is plotted against time. At the arrow (time 0), the patch clamp was switched from the voltage clamp to the current clamp mode and stimulation of MF was interrupted for 5 min. The traces above the graph show 7 consecutive responses (upper traces) and average of all responses (including failures, lower traces) in control and 15 min after switching back from current clamp to voltage clamp mode. (*B*) Mean EPSC amplitude before and 15 min after switching from voltage clamp to current clamp mode for five cells treated with the same protocol as in *A*. (*C*) Temporal specificity of the correlated activity required for LTP induction. During the pairing protocol, a delay of 0–5 s was introduced between GDP rise time and synaptic stimulation. Each symbol represents the mean percentage increase of EPSCs amplitude as a function of the delay for the number of cells indicated (into brackets). Small bars represent the average of all open circles in a column. Note that the maximum potentiating effect was achieved when pre- and postsynaptic signals were coincident.

revealed that input 1 (expressing paired-pulse facilitation) originated from MF because it was blocked LAP-4 and picrotoxin (Fig. 3*A*), whereas input 2 originated from a GABAergic interneuron because it was insensitive to LAP-4 (25, 30) but was blocked by picrotoxin (Fig. 3*B*). Similar results were obtained in six cells. However, in two cases "pairing" resulted in LTP that did spread to the other nonstimulated input converging into the same cell (data not shown). Spreading of LTP to neighboring synapses is a well known phenomenon (31–33) that may provide a cooperative mechanism for establishing multiple converging inputs in the developing hippocampus. The degree of spreading may be related to the particular geometry of the synapses under examination that, during postnatal development, undergo continuous remodeling. In Fig. 3*C*, the mean percentage values of EPSC amplitude for all paired and unpaired inputs are represented. Whereas paired inputs exhibited a significant increase in the amplitude of synaptic responses (176 ± 31%; $n = 26$; $P < 0.01$), unpaired inputs were almost unaltered (125 ± 34%; $n = 22$; $P > 0.5$).

Pairing-Induced LTP Depends on the Rise in Calcium Concentration in the Postsynaptic Cell Through Voltage-Dependent Calcium Channels (VDCC). A common trigger for activity-dependent long-lasting modifications of synaptic strength at both glutamatergic (34, 35) and GABAergic synapses (36) is a postsynaptic rise in intracel-

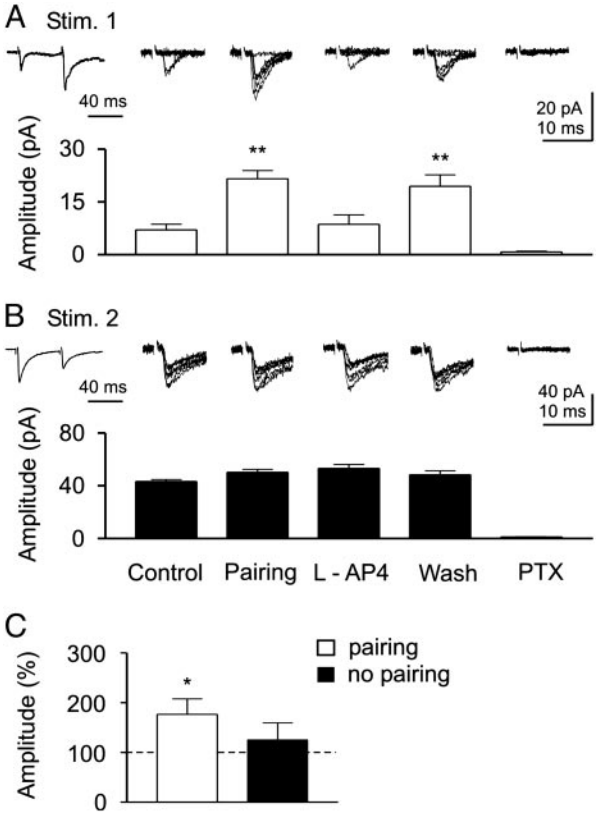

Fig. 3. Pairing-induced homosynaptic potentiation. (*A* and *B*) Two different inputs converging into the same CA3 pyramidal neuron were alternatively activated at 0.2 Hz with paired stimuli delivered at 50-ms intervals (see diagram of Fig. 1*A*). Stim. 1 localized on stratum lucidum induced synaptic responses exhibiting paired-pulse facilitation typical for the MF input, whereas Stim. 2 localized on stratum radiatum induced synaptic responses exhibiting paired-pulse depression. Traces on the left represent the average of 60 responses obtained in control by Stim. 1 (*A*) or by Stim. 2 (*B*). Pairing GDPs with Stim. 1 induced a persistent increase in synaptic efficacy of input 1 but not input 2. Each column represents mean amplitudes of EPSC evoked by activation of Stim. 1 (white columns, *A*) or Stim. 2 (black columns, *B*) in different experimental conditions. Above the columns are six consecutive individual traces obtained in respective experimental conditions. Pharmacological identification (LAP-4) revealed that input 1 originated from MF, whereas input 2 originated from a non-MF input (presumably GABAergic interneuron; note paired-pulse depression and suppression by PTX). (*C*) Mean EPSC amplitude for all paired or unpaired inputs ($n = 29$ and 23, respectively). *, $P < 0.01$; **, $P < 0.001$.

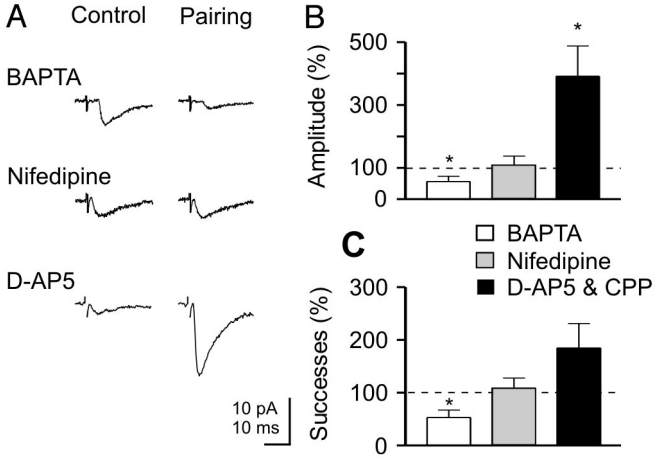

Fig. 4. Pairing-induced potentiation needs a rise of intracellular calcium concentration in the postsynaptic cell via voltage-dependent calcium channels. (*A*) EPSCs evoked by MF stimulation in control conditions and 15 min after pairing in the presence of intracellular BAPTA (20 μM), extracellular nifedipine (10 μM), or D-AP5 (50 μM). Each response is the average of 30 traces. (*B* and *C*) Pairing-induced changes in the mean amplitude (*B*) and mean number of successes (*C*) of MF-EPSCs expressed as percentage of controls for all cells tested (with BAPTA, $n = 9$; nifedipine, $n = 7$; and D-AP5, $n = 4$; or CPP, $n = 2$). *, $P < 0.01$.

lular calcium concentration. In the following experiments, we tested whether a rise of postsynaptic calcium during GDPs is responsible for pairing-induced LTP at MF–CA3 connections. In cells loaded with the calcium chelator BAPTA (20 mM; $n = 9$, see example of Fig. 4*A*), the pairing procedure produced a long-lasting and significant decrease of synaptic efficacy that persisted for up to 30 min. The summary data of Fig. 4 *B* and *C* show a significant reduction in the mean peak amplitude current (to 56 ± 17% relative to control; $P < 0.001$) and in the percentage of successes (53 ± 14%; $P < 0.01$). These experiments suggest that pairing-induced LTP depend on the increase in intracellular calcium concentration in the postsynaptic cell. As predicted by the relationship between activity-dependent increase in postsynaptic calcium and the polarity of synaptic modifications, high levels of calcium would result in LTP, whereas low levels would result in LTD (37, 38).

A rise of intracellular calcium concentration during GDPs may occur via NMDA receptors or via VDCC (12). To identify the source of calcium responsible for GDP-induced LTP, additional experiments were performed in the presence of NMDA receptor antagonists (CPP, $n = 2$ or D-AP5, $n = 4$) or the VDCC blocker nifedipine ($n = 7$). Whereas CPP (20 μM) or D-AP5 (50 μM) failed to prevent LTP (after pairing the mean EPSC amplitude was 391 ± 97%; $P < 0.05$; the mean successes rate was 185 ± 46%, relative to control), nifedipine (10 μM) blocked it (in five of seven cells; Fig. 4 *A–C*). In the presence of nifedipine, the mean peak amplitude of MF-evoked synaptic currents after pairing was not significantly different from controls (111 ± 26%; $P > 0.5$) and so were changes in the number of successes (108 ± 19%; $P > 0.5$). This indicates that, early in postnatal life, calcium rise through VDCC is the common trigger for activity-dependent changes in synaptic strength. It is worth noting that nifedipine, CPP, and D-AP5 did not alter the shape or the amplitude of GDPs (data not shown; see also ref. 3).

Discussion

The present experiments clearly show that, during the first postnatal week, correlated pre- (MF) and postsynaptic (GDPs) activity persistently enhances synaptic strength at MF–CA3 connections. They also demonstrate that, at this developmental stage, GABA is the main neurotransmitter released from the MF (21, 22). That granule cells from the DG may corelease GABA and glutamate early in postnatal life was already known (21). The present results further strengthen this point, showing that, before day 6, monosynaptic MF–CA3 responses are mainly GABAergic because DNQX-sensitive glutamatergic currents could be seen only after increasing stimulus strength two or more times. This finding is consistent with the sequential expression of functional GABA and glutamatergic synapses found in the hippocampus at early developmental stages (6, 27).

As in many other forms of synaptic plasticity (34), a transient rise of intracellular calcium was required for LTP induction. However, in contrast to previous studies, in the present experiments GABA itself provided the depolarization needed to activate VDCC. It has been shown that repeated bursts of action potentials, applied at low frequency to CA3 pyramidal cells, are able to induce LTP at immature interneuron–CA3 synapses only in the presence of NMDA receptor antagonists (36, 39). In the

absence of NMDA antagonists, the same conditioning stimuli will produce LTD (39, 40). In our case, LTP induction was independent of NMDA receptor activation, but relied on the activation of postsynaptically localized VDCCs. In older animals, induction of LTP at MF synapses was shown to be independent of postsynaptic activation (41, 42). However, like in the present experiments, under certain conditions, MF–LTP may involve a rise of calcium in the postsynaptic cell (43–45). This suggests that, at MF synapse, different forms of LTP may coexist. Moreover, the possibility to induce MF–LTP in juvenile animals with conditioning intracellular depolarizing pulses (46) is also in line with the present observations. Although LTP induction was clearly dependent on postsynaptic events, its expression was mainly presynaptic, as suggested by the pairing-induced decrease in failures rate, in paired-pulse facilitation, and the increase in CV^{-2}, all traditional indices of changes in presynaptic release probability. Although changes in failure rate and CV^{-2} could result from the insertion of new receptors on the subsynaptic membrane in previously silent synapses (47), this explanation is difficult to reconcile with the reduction of the paired-pulse ratio. Moreover, the appearance of synaptic responses in apparently "silent" neurons containing postsynaptic receptors ("presynaptically silent" synapses) is consistent with pairing-induced increase in release probability. Therefore, our data favor the possibility of concomitant presynaptic changes in the release machinery. It is also possible that the initial pairing-induced increase in intracellular calcium trigger coordinated pre- and postsynaptic modifications, thus promoting the cross talk between pre and postsynaptic elements. Whatever the mechanisms, GDPs appear to be effective in "unsilencing" silent connections and for strengthening those with low probability of transmitter release (23, 28–29). They might also be instructive in promoting synapse development in those neurons "silent" because of the lack of presynaptic specialization (48).

Hence, during development, GABA-mediated spontaneous membrane oscillations provide a significant induction mechanism for enhancing synaptic efficacy at emerging synapses in a Hebbian way. Whether this may contribute to sculpt neuronal circuits, as demonstrated in the developing visual system and spinal cord (49), remains to be determined. Later in development, when the degree of functional connections is sufficiently high, GDPs would be replaced by more subtle types of signal synchronization such as theta or gamma activity characteristic of the adult network (2, 50).

We are grateful to John Nicholls for carefully reading the manuscript and to Renato Tomizza for technical assistance. This work was supported by grants from Ministero dell'Istruzione dell'Università e della Ricerca (MIUR), from the European Union (Project 503221; to E.C.), International Association for the Promotion of Cooperation with Scientists from the New Independent States of the Former Soviet Union (INTAS) (to E.C. and L.L.V.), the Russian Foundation for Basic Research (RFBR) and Wellcome Trust (to L.L.V.), and the RFBR (to V.F.S.).

1. Ben-Ari, Y., Cherubini, E., Corradetti, R. & Gaiarsa, J. L. (1989) *J. Physiol.* **416,** 303–325.
2. Leinekugel, X., Khazipov, R., Cannon, R., Hirase, H., Ben-Ari, Y. & Buzsaki, G. (2002) *Science* **296,** 2049–2052.
3. Bolea, S., Avignone, E., Berretta, N., Sanchez-Andres, J. V. & Cherubini, E. (1999) *J. Neurophysiol.* **81,** 2095–2102.
4. Cherubini, E., Gaiarsa, J. L. & Ben-Ari, Y. (1991) *Trends Neurosci.* **14,** 515–519.
5. Ben-Ari, Y., Khazipov, R., Leinekugel, X., Caillard, O. & Gaiarsa, J. L. (1997) *Trends Neurosci.* **20,** 523–529.
6. Ben-Ari, Y. (2002) *Nat. Rev. Neurosci.* **3,** 728–739.
7. Delpire, E. (2000) *News Physiol. Sci.* **15,** 309–312.
8. Rivera, C., Voipio, J., Payne, J. A., Ruusuvuori, E., Lahtinen, H., Lamsa, K., Pirvola, U., Saarma, M. & Kaila, K. (1999) *Nature* **397,** 251–255.
9. Ganguly, K., Schineder, A. F., Wong, S. T. & Poo, M. M. (2001) *Cell* **105,** 521–532.
10. Owens, D. F. & Kriegstein, A. R. (2002) *Nat. Rev. Neurosci.* **3,** 715–727.
11. Leinekugel, X., Tseeb, V., Ben-Ari, Y. & Bregestovski, P. (1995) *J. Physiol.* **487,** 319–329.
12. Leinekugel, X., Medina, I., Khalilov, I., Ben Ari, Y. & Khazipov, R. (1997) *Neuron* **18,** 243–255.
13. Garaschuk, O., Hanse, E. & Konnerth, A. (1998) *J. Physiol.* **507,** 219–236.
14. Yuste, R. & Katz, L. C. (1991) *Neuron* **6,** 333–344.
15. Wong, R. O., Chernjavsky, A., Smith, S. J. & Shatz, C. J. (1995) *Nature* **374,** 716–718.
16. Spitzer, N. C., Lautermilch, N. J., Smith, R. D. & Gomez, T. M. (2000) *BioEssays* **22,** 811–817.
17. Garaschuk, O., Linn, J., Eilers, J. & Konnerth, A. (2000) *Nat. Neurosci.* **3,** 452–459.
18. Zhang, L. I. & Poo, M. M. (2001) *Nat. Neurosci. Suppl.* **4,** 1207–1214.
19. Katz, L. C. & Shatz, C. J. (1996) *Science* **274,** 1133–1138.
20. Amaral, D. G. & Dent, J. A. (1981) *J. Comp. Neurol.* **195,** 51–86.
21. Walker, M. C., Ruiz, A. & Kullmann, D. M. (2001) *Neuron* **29,** 703–715.
22. Gutierrez, R., Romo-Parra, H., Maqueda, J., Vivar, C., Ramirez, M., Morales, M. A. & Lamas, M. (2003) *J. Neurosci.* **23,** 5594–5598.
23. Gasparini, S., Saviane, C., Voronin, L. L. & Cherubini, E. (2000) *Proc. Natl. Acad. Sci. USA* **97,** 9741–9746.
24. Yamamoto, C., Sawada, S. & Takada, S. (1983) *Exp. Brain Res.* **51,** 128–134.
25. Semyanov, A. & Kullmann, D. M. (2000) *Neuron* **25,** 663–672.
26. Salin, P. A., Scanziani, M., Malenka, R. C. & Nicoll, R. A. (1996) *Proc. Natl. Acad. Sci. USA* **93,** 13304–13309.
27. Hennou, S., Khalilov, I., Diabira, D., Ben-Ari, Y. & Gozlan, H. (2002) *Eur. J. Neurosci.* **16,** 197–208.
28. Maggi, L., Le Magueresse, C., Changeux, J.-P. & Cherubini, E. (2003) *Proc. Natl. Acad. Sci. USA* **100,** 2059–2064.
29. Voronin, L. L. & Cherubini, E. (2003) *Neuropharmacol*ogy **45,** 439–449.
30. Scanziani, M., Gahwiler, B. H. & Charpak, S. (1998) *Proc. Natl. Acad. Sci. USA* **95,** 12004–12009.
31. Engert, F. & Bonhoeffer, T. (1997) *Nature* **388,** 279–284.
32. McMahon, L. L. & Kauer, J. (1997) *Neuron* **18,** 295–305.
33. Tao, H. W, Zhang, L. I., Engert, F. & Poo, M. (2001) *Neuron* **31,** 569–580.
34. Bliss, T. V. P. & Collingridge, G. L. (1993) *Nature* **361,** 31–39.
35. Malenka, R. C. & Nicoll, R. A. (1999) *Science* **285,** 1870–1874.
36. Caillard, O., Ben-Ari, Y. & Gaiarsa, J. L. (1999) *J. Physiol.* **518,** 109–119.
37. Lisman, J. E. (2001) *J. Physiol.* **532,** 285.
38. Cho, K., Aggleton, J. P., Brown, M. W. & Bashir, Z. I. (2001) *J. Physiol.* **532,** 459–466.
39. Gaiarsa, J. L., Caillard, O. & Ben-Ari, Y. (2002) *Trends Neurosci.* **25,** 564–570.
40. McLean, H. A., Caillard, O., Ben-Ari, Y. & Gaiarsa, J. L. (1996) *J Physiol.* **496,** 471–477.
41. Nicoll, R. A. & Malenka, R. C. (1995) *Nature* **377,** 115–118.
42. Mellor, J. & Nicoll, R. A. (2001) *Nat. Neurosci.* **4,** 125–126.
43. Urban, N. N. & Barrionuevo, G. (1996) *J. Neurosci.* **16,** 4293–4299.
44. Yeckel, M. F., Kapur, A. & Johnston, D. (1999) *Nat. Neurosci.* **2,** 625–633.
45. Wang, J., Yeckel, M. F., Johnston, D. & Zucker, R. S. (2003) *J. Neurophysiol.*, in press
46. Berretta, N., Rossokhin, A. V., Cherubini, E., Astrelin, A. V. & Voronin, L. L. (1999) *Neuroscience* **93,** 469–477.
47. Kullmann, D. M. (2003) *Philos. Trans. R Soc. London B* **358**, 727–733.
48. Demarque, M., Represa, A., Becq, H., Khalilov, I., Ben-Ari, Y. & Anikstejn, L. (2002) *Neuron* **36,** 1051–1061.
49. Feller, M. B. (1999) *Neuron* **22,** 653–656.
50. Buzsaki, G. & Chrobak, J. J. (1995) *Curr. Opin. Neurobiol.* **5,** 504–510.